Revised manuscript prepared for the proceedings of the conference Migration '07 (Radiochimica Acta)

Solubility of Zr(IV), Th(IV) and Pu(IV) hydrous oxides in $CaCl_2$ solutions and the formation of ternary Ca-M(IV)-OH complexes

M. Altmaier[1] *, V. Neck[1] *, Th. Fanghänel[1,2]

[1] Forschungszentrum Karlsruhe, Institut für Nukleare Entsorgung, PO Box 3640, D-76021 Karlsruhe, Germany

[2] European Commission, Joint Research Centre, Institute for Transuranium Elements, PO Box 2340, D-76125 Karlsruhe, Germany

Keywords: Zirconium / Thorium / Plutonium / Ternary Ca-M(IV)-OH complexes / Solubility / Thermodynamics / SIT /

Summary

The solubility of Zr(IV), Th(IV) and Pu(IV) hydrous oxides is investigated at 22 ± 2°C in alkaline 0.1 - 4.5 M $CaCl_2$ solutions. Further studies are performed with Zr(IV) over the entire pH range in NaCl and $CaCl_2$ media, and with Zr(IV) and Th(IV) in alkaline $Ca(ClO_4)_2$ solutions. The comparison of Zr(IV) data in different ionic media (NaCl, $NaClO_4$, $CaCl_2$ and $Ca(ClO_4)_2$) of similar ionic strength shows that the solubility in the acidic and neutral pH range is not affected by strong interactions between the aqueous M(IV) species and the medium ions. However, in alkaline $CaCl_2$ and $Ca(ClO_4)_2$ solutions the formation of ternary Ca-M(IV)-OH complexes causes unexpectedly high solubilities of Zr(IV) at pH_c = 10 - 12 and $[Ca^{2+}]$ > 0.05 M and of Th(IV) at pH_c = 11 - 12 and $[Ca^{2+}]$ > 0.5 M. The dependence of the Zr(IV) and Th(IV) solubilities on the H^+ and $CaCl_2$ concentrations shows that the complexes $Zr(OH)_6^{2-}$ and $Th(OH)_8^{4-}$ with an unusual large number of OH^- ligands are stabilized by the formation of associates or ion pairs with Ca^{2+} ions. The SIT is used to derive equilibrium constants at zero ionic strength for the complexes $Zr(OH)_6^{2-}$ (in calcium-free solutions), $Ca_2[Zr(OH)_6]^{2+}$, $Ca_3[Zr(OH)_6]^{4+}$ and $Ca_4[Th(OH)_8]^{4+}$. In analogous studies with Pu(IV) hydrous oxide, the solubility increasing effect of ternary complex formation with Ca^{2+} ions is only observed at $CaCl_2$ concentrations above 2 M.

---

* Corresponding authors. E-mail address: altmaier@ine.fzk.de, neck@ine.fzk.de

1. Introduction

The solubility and aqueous speciation of tetravalent actinides in chloride solutions is of particular interest for the storage of nuclear waste in underground salt mines. As the corrosion of cementitious waste packages in $MgCl_2$ solution can lead to alkaline $CaCl_2$ solutions, we have studied the solubility of Zr(IV), Th(IV) and Pu(IV) oxyhydroxide precipitates which may also be called hydrous oxide, $MO_2{\cdot}xH_2O(s)$, or hydroxide, $M(OH)_4(s)$. The literature on the solubility and hydrolysis of tetravalent actinides and Zr(IV) in acidic to alkaline alkali salt media is extensively discussed in recent reviews [1 - 4]. The low solubilities measured after ultrafiltration or ultracentrifugation in carbonate-free solutions of pH 6 - 13 (log [Zr] = - 7.5 ± 0.8 [5,6], log [Th] = - 8.5 ± 0.6 [1,7], and log [Pu(IV)] = - 10.4 ± 0.5 [1,8]) are usually described by equilibria with neutral aqueous complexes $M(OH)_4(aq)$ or $M_m(OH)_{4m}(aq)$. Numerous solubility studies with An(IV) hydrous oxides (An = Th, U, Np, Pu) in alkali hydroxide solutions up to pH 14 show no indication for the formation of anionic hydroxide complexes $An(OH)_n^{4-n}$ with $n > 4$ (*c.f.*, discussion in [1,2,4]). The solubility increase observed in a few studies with U(IV), Np(IV) and Pu(IV) in highly basic solutions [9 - 11] may be caused by the interference of carbonate or by species at higher oxidation states; the proposed data for $An(OH)_5^-$ or $An(OH)_6^{2-}$ complexes are therefore not accepted in the database of the OECD / Nuclear Energy Agency (NEA-TDB). Solely the formation of $Zr(OH)_6^{2-}$ at high hydroxide concentrations (e.g. in 1 - 10 M NaOH) [5,12,13] is considered to be proven [3].

Although the alkalinity of $CaCl_2$ solutions is limited by the solubility of calcium hydroxide or hydroxychlorides ($pH_c \leq 12$ in 0.1 - 4.5 M $CaCl_2$) we measured unexpectedly high solubilities with Zr(IV) and Th(IV) hydrous oxides. The concentrations at $pH_c = 11$ to 12 partly exceed 10^{-3} $mol{\cdot}L^{-1}$ which is sufficient to investigate the saturated solutions by extended x-ray absorption fine structure spectroscopy (EXAFS) [14]. A part of our solubility data was briefly discussed as background of this EXAFS study. In the present paper the solubility in $CaCl_2$ solution and its dependence on the H^+ and Ca^{2+} concentrations are discussed in detail in comparison with data in NaCl, $NaClO_4$ and $Ca(ClO_4)_2$ media.

The specific ion interaction theory (SIT) recommended in the NEA-TDB reviews [2 - 4] is used for ionic strength corrections. According to the SIT the activity coefficients γ_i of aqueous species i are given by

$$\log \gamma_i = - z_i^2 D + \Sigma \varepsilon_{ij} m_j \qquad (1)$$

where z_i is the charge of ion i, ε_{ij} is the interaction parameter for a pair of oppositely charged ions, m_j (mol/kg H_2O) is the molal concentration of ion j, and D is the Debye-Hückel term ($D = 0.509\sqrt{I_m} / (1 + 1.5 \sqrt{I_m})$ at 25°C). I_m is the molal ionic strength. Conversion factors to calculate the molal concentrations m_i (mol/kg H_2O) from the molar concentrations c_i (M = mol/L), water activities a_w and ion interaction coefficients are taken from the NEA-TDB [2,3] as far as available. The value of $\varepsilon(Ca^{2+}, OH^-) = -0.45 \pm 0.03$ $kg{\cdot}mol^{-1}$ is derived from the

values of log γ_{OH^-} in 0 - 5 m $CaCl_2$ solution, which are calculated with the widely accepted data set and ion interaction (Pitzer) parameters reported by Harvie et al. [15] for the seawater salt system (HMW model). This does not cause inconsistencies because the values of log γ_{H^+} in 0 - 5 m $CaCl_2$ solution calculated with the SIT agree well with those based on the HMW model. The strongly negative interaction coefficients for the couple (Ca^{2+}, OH^-) account for the effect of ion-paring, *i.e.*, the HMW model does not explicitly include the species $CaOH^+$.

2. Experimental

Chemicals and analytical methods. Solid $CaCl_2{\cdot}2H_2O$ (p.a.), $Ca(OH)_2$(p.a.), and NaCl (p.a.) were obtained from Merck, $Ca(ClO_4)_2{\cdot}4H_2O$ from Aldrich. The stoichiometric composition of $CaCl_2{\cdot}2H_2O$ (p.a.), *i.e.*, the water content was confirmed by chloride analysis. The H^+ standard solutions in NaCl and $CaCl_2$ used for the calibration of the pH electrodes and for adjusting pH in the solubility experiments in acidic solutions were prepared with HCl titrisol (Merck). For the studies in alkaline 0.1, 0.2, 0.5, 1.0, 2.0, and 4.5 M $CaCl_2$, matrix solutions with maximum pH values were prepared by equilibration with solid $Ca(OH)_2$(cr) for about one week. In 4.5 M $CaCl_2$ the solid $Ca(OH)_2$(cr) transforms into $Ca_2(OH)_2Cl_2{\cdot}H_2O$(cr) within a few days. The solid calcium hydroxide or hydroxychloride was removed by ultrafiltration and $CaCl_2$ matrix solutions at lower pH values were obtained by dilution with the corresponding $CaCl_2$ solutions. All solutions were prepared with ultrapure water purified with a Milli-Q-academic (Millipore) apparatus and purged with Ar before they were used.

The Zr and Th concentrations were determined by ICP-MS (ELAN 6100, Perkin Elmer) at a background of about 0.005 ppb Zr-90 and 0.002 ppb Th-232. Depending on the chloride concentration the aliquots for ICP-MS analysis (acidified in 2% HNO_3) have to be diluted 1:10 to 1:100. Accordingly, the detection limit for Zr and Th in the original solutions varied from 10^{-9} to 10^{-8} mol·L^{-1}. The concentration of plutonium (99.4 wt.% Pu–242, 0.58 wt.% Pu-239, 0.005 wt.% Pu-238 and 0.005 wt.% Pu-241) was determined by liquid scintillation counting with a TriCarb 2500 TR/AB (Canberra-Packard); detection limit: 10^{-10} M.

Solid phases and solubility measurements. Amorphous precipitates of $ZrO_2{\cdot}xH_2O$(s) and $ThO_2{\cdot}xH_2O$(s) were prepared by slow addition of 0.1 M NaOH (carbonate-free, Baker) to about 0.02 M solutions of $Th(NO_3)_4{\cdot}6H_2O$(p.a.) (Merck) and $ZrOCl_2{\cdot}xH_2O$ (Aldrich), respectively. The precipitates were washed several times with water and stored for several weeks to minimize aging effects during the solubility experiments. The Th(IV) precipitate was x-ray amorphous while powder diffraction pattern of the Zr(IV) precipitate showed the most intense peaks of monoclinic ZrO_2(cr) (JCPDS file 37-1484) as weak broad bands. The solubility study with hydrous Pu(IV) oxide, PuO_{2+x}(am,hyd) containing about 0.5 % of oxidized Pu, was performed with the solid used in our recent study in 0.1 M NaCl [16]. All solubility experiments were performed in polyethylene vials. Appropriate amounts of the solid hydrous oxides were suspended in 10 - 50 mL of the matrix solution and stored at 22 ±

2°C in an argon glove box. After equilibration for 7 - 198 days the samples were analyzed for H^+ and metal ion concentrations. The latter were measured after ultrafiltration (Pall Life Sciences, 10 kD, pore size about 1.5 nm) or ultracentrifugation for 60 minutes at 90000 rpm (Beckman XL-90, mean relative centrifugal force: ca. $5 \cdot 10^5$ g).

pH measurements. The molar H^+ concentrations ($pH_c = -\log c_{H^+}$) in NaCl and $CaCl_2$ solutions were determined with combination pH electrodes (type ROSS, Orion) as described previously and more detailed for analogous pH measurements in NaCl and $MgCl_2$ solutions [17]. Calibration against pH (activity scale) standard buffers (pH 1 - 10, Merck) yields operational "measured" pH_{exp} values in salt solutions of ionic strength I > 0.1 mol/kg, with $pH_c = pH_{exp} + A_c$ and $pH_m = pH_{exp} + A_m$ for the molal H^+ concentrations ($pH_m = -\log m_{H^+}$). The parameter A includes the individual activity coefficient γ_{H^+} and a contribution ΔE_j from the variation of the liquid junction potential E_j when measuring dilute pH buffer solutions for calibration and saline test solutions. The experimental values of A_c, determined from pH_{exp} in 0.1 - 4.5 M $CaCl_2$ standard solutions containing 0.001 - 0.1 M HCl, and the corresponding values of A_m can be expressed empirically by the following polynomials:

$$A_c = -0.1044 + 0.4014\, c_{CaCl2} + 0.0384\, (c_{CaCl2})^2$$
$$A_m = -0.1176 + 0.4308\, m_{CaCl2} + 0.0096\, (m_{CaCl2})^2$$

The H^+ concentrations measured in $CaCl_2$ solutions equilibrated with solid $Ca(OH)_2$(cr) or $Ca_4(OH)_6Cl_2 \cdot 13H_2O$(s) agree well with calculated values based on the thermodynamic data and parameters reported by Harvie et al. [15] (*c.f.*, Fig. 1). For pH measurements in 0.2, 1.0 and 2.0 M $Ca(ClO_4)_2$ solutions (m_{Ca} = 0.204, 1.088 and 2.397 mol/kg [18]) the junction electrolyte was replaced by 3.0 M NaCl; A_m = 0.05, 0.47 and 1.00, respectively.

3. Results and discussion

3.1. Solubility of Zr(IV) hydrous oxide in different ionic media

The experimental solubility data measured with Zr(IV) hydrous oxide in NaCl and $CaCl_2$ solutions are shown in Fig. 2 over the entire pH range, together with literature data in $NaClO_4$ and a few additional data in alkaline $Ca(ClO_4)_2$ solutions. The comparison for data at equal or similar ionic strength of I = 0.5 - 0.6 M (Fig. 2a), I = 1.0 - 1.5 M (Fig. 2b), and I = 3.0 M (Fig. 2c) allows to distinguish between the influence of the medium anion (either Cl^- or non-complexing ClO_4^-) and the medium cation (either Ca^{2+} or Na^+). XRD pattern taken from the solid phases in acidic 3.0 M NaCl and alkaline 2.0 M $CaCl_2$ did not show any changes compared to the initial solid.

Acidic solutions. The solubilities at pH_c = 1 - 3 decrease with a constant slope of -3 (log [Zr] vs. pH_c). Our data in NaCl and $CaCl_2$ solutions of similar ionic strength are nearly on the same lines (Figs. 2a and 2c). The discrepancies between the data of Ekberg et al. [5] and

Sasaki et al. [6] in 1.0 M $NaClO_4$ (Fig. 2b) are typical for differences in the degree of crystallinity or particle size of the solid phase, due to somewhat different preparation and aging conditions. These effects cause much larger differences than the variation of the ionic media or ionic strength. The curves calculated for the same solid in $NaClO_4$ and NaCl solutions (*i.e.*, with the same solubility product at I = 0) differ only slightly at higher ionic strength.

Near neutral pH range. At $pH_c > 3$, up to $pH_c = 12 - 13$ in NaCl and $NaClO_4$ media and up to $pH_c = 10$ in $CaCl_2$ solutions, the Zr concentration is at a constant level, independent of the ionic medium and independent of whether the bulk solid phase is more or less crystalline. Recent data determined by Cho et al. [19] for fresh, colloidal $Zr(OH)_4$(am) particles at pH > 6 are in the range of solubilities measured with aged precipitates after ultrafiltration or ultracentrifugation: log [Zr] = - 7.4 ± 0.6 [5], - 7.6 ± 0.9 [6] or - 7.8 ± 0.7 (present work). This Zr concentration is caused by neutral aqueous $Zr_m(OH)_{4m}$(aq) species in equilibrium with small amorphous particles included in the bulk solid or with an amorphous hydrated surface (*c.f.*, discussion for Th(IV) and U(IV) oxides of different crystallinity [4,20,21]). The large scatter of solubility data at these low concentrations (shadowed grey areas in Fig. 2) arises from analytical problems, e.g., insufficient separation of colloidal species or sorption effects during phase separation.

Alkaline solutions. At $pH_c > 13$ in NaCl and $NaClO_4$ media the solubility curves (log [Zr] vs. pH_c) show a distinct increase with a slope of 2, due to the formation of the complex $Zr(OH)_6^{2-}$ [3]. In $CaCl_2$ solutions, this solubility increase with a slope of 2 is much more pronounced and already observed at significantly lower pH_c values in the range 10 - 12. The solubility in 0.5 and 1.0 M NaCl/NaOH is similar to that in 1.0 M $NaClO_4$/NaOH but orders of magnitude lower than those in $CaCl_2$ solutions with similar chloride concentrations. Moreover, the zirconium concentrations measured after 14 and 27 days in 0.2 and 1.0 M $Ca(ClO_4)_2$ are close to the solubilities in 0.2 and 1.0 M $CaCl_2$ (*c.f.*, Figs. 2a and 2c). This clearly demonstrates that the solubility increase is not caused by complex formation with chloride ions but by strong interaction with Ca^{2+} (ion association or ion pair formation). This conclusion is further corroborated by EXAFS measurements with a couple of saturated Zr(IV) solutions in 0.5, 1.0 and 2.0 M $CaCl_2$ at $pH_c = 11.6 - 12.0$ [14]. The EXAFS spectra clearly show a second coordination shell coming from calcium backscatter atoms. There is no indication of Zr-Zr backscattering like in Zr(IV) oligomers or oxyhydroxide colloids. The presence of chloride ligands can also be ruled out. The coordination numbers ($N_O = 6.6 \pm 1.2$, $N_{Ca} = 2.7 \pm 0.6$) and distances ($R_{Zr-O} = 2.20 \pm 0.02$ Å, $R_{Zr-Ca} = 3.38 \pm 0.02$ Å) and the relatively small Debye-Waller factors indicate the presence of a single species $Ca_3[Zr(OH)_6]^{4+}$ where the Ca^{2+} ions are bound to the edges of a distorted $Zr(OH)_6^{2-}$ octahedron which possibly includes an additional H_2O ligand [14].

3.1.1. Thermodynamic model for the solubility and hydrolysis of Zr(IV) at pH 0 - 10

The hydrolysis of the Zr^{4+} ion has been critically discussed in a recent NEA-TDB review [3] which analyzed potentiometric, ion exchange, solvent extraction, and solubility data and derived a chemical model from an overall fit. Besides the mononuclear species $Zr(OH)_n^{4-n}$ with n = 0, 1, 2, 4 and 6 the model included two trimers, $Zr_3(OH)_4^{8+}$ and $Zr_3(OH)_9^{3+}$, and the tetramers $Zr_4(OH)_8^{8+}$, $Zr_4(OH)_{15}^{+}$, and $Zr_4(OH)_{16}(aq)$. However, the exact stoichiometries of the oligomeric species dominant in acidic solutions are not well ascertained, e.g.: "*The species $Zr_3(OH)_9^{3+}$ has been introduced to increase the quality of the global fit of the hydrolysis data. This species has not yet been identified or proposed in the experimental literature.*" [3]. The same holds for $Zr_4(OH)_{15}^{+}$ and $Zr_4(OH)_{16}(aq)$. In a very recent study based on nanoelectrospray mass-spectrometry, Walther et al. [22] detected a much large variety of oligomeric species $Zr_m(OH)_n^{z+}$, mainly with m = 4, 5, and 8 and charges decreasing continuously from z = +15 to +2 when pH_c is increased from 0 to 3 at a given Zr concentration in the range $[Zr]_{tot} = 10^{-3}$ - 10^{-2} M. The authors found no evidence for the formation of trimers under their experimental conditions. Anyway, both the NEA-TDB model and the results of Walther et al. [22] show that the speciation along the solubility of Zr(IV) hydroxides or hydrous oxides is not dominated by mononuclear hydroxide complexes but by oligomers. Even somewhat larger polymers might be present [6].

In order to calculate the solubility product of $ZrO_2{\cdot}xH_2O(s)$ from the data at $pH_c < 3$ we have adopted the hydrolysis scheme proposed in the NEA-TDB review [3]. The equilibrium constants and ion interaction (SIT) coefficients are listed in Tables 1 and 2. Unknown SIT coefficients $\varepsilon(Zr_m(OH)_n^{z+}, Cl^-)$ are estimated from an empirical relation, $\varepsilon(M^{z+}, Cl^-) = 0.38\ \varepsilon(M^{z+}, ClO_4^-) \pm 0.1$ kg·mol^{-1}, valid for all metal ions M^{z+} with z = 1 - 4 [23] and also for thorium hydroxide complexes $Th_m(OH)_n^{z+}$ with z = 0 - 10 [4]. In agreement with the observed slope of -3 for log [Zr] vs. pH_c, the trinuclear complex $Zr_3(OH)_9^{3+}$ is calculated to be the dominant species in the saturated solutions at pH_c = 1 - 3. All other Zr(IV) species give very minor contributions to the total Zr concentrations. Hence the solubility in this pH range, *i.e.*, the dissolution of $Zr(OH)_4(s)$ and the subsequent hydrolysis of Zr^{4+}:

$$Zr(OH)_4(s) + 4\ H^+ \Leftrightarrow Zr^{4+} + 4\ H_2O \qquad (\log{*}K_{s,0}) \qquad (2)$$

$$3\ Zr^{4+} + 9\ H_2O \Leftrightarrow Zr_3(OH)_9^{3+} + 3\ H^+ \qquad (\log{*}\beta_{3,9}) \qquad (3)$$

is dominated by the reaction

$$3\ Zr(OH)_4(s) + 3\ H^+ \Leftrightarrow Zr_3(OH)_9^{3+} + 3\ H_2O \qquad (4)$$

The equilibrium constant for reaction (4) and the contribution of the trimer $Zr_3(OH)_9^{3+}$ to the the Zr concentration in solution ($[Zr]_{(3,9)} = 3\ [Zr_3(OH)_9^{3+}]$) are given by Eqs. (5) and (6):

$$\log{*}K_{s,(3,9)} = 3\ \log{*}K_{s,0} + \log{*}\beta_{3,9} = \log\ [Zr_3(OH)_9^{3+}] - 3\ \log\ [H^+] \qquad (5)$$

$$\log [Zr]_{(3,9)} = \log (3) + 3 \log^* K_{s,0} + \log^* \beta_{3,9} + 3 \log [H^+]$$
$$= \log (3) + 3 \log^* K°_{s,0} + \log^* \beta°_{3,9} + 3 \log [H^+]$$
$$+ \Delta z^2 D - \varepsilon(Zr_3(OH)_9^{3+}, Cl^-)\, m_{Cl^-} + 3\, \varepsilon(H^+, Cl^-)\, m_{Cl^-} - 3 \log a_w \qquad (6)$$

where $\log^* K_{s,0}$ and $\log^* \beta_{3,9}$ are conditional equilibrium constants in a given medium and those with index "°" refer to the standard state. The Debye-Hückel term Δz^2 D with $\Delta z^2 = 6$ for reaction (4) is given by the SIT (Eq. (1)) and $\log^* \beta°_{3,9} = 12.19 \pm 0.08$ [3]. The values of $\varepsilon(H^+, Cl^-)$ and water activity a_w are tabulated in [2]. (The concentrations $\log [Zr]_{(m,n)}$ of the other species (*m*,*n*) are given by analogous equations.) The unknown parameters in Eq. (6), $\log^* K°_{s,0}$ (at I = 0) and $\varepsilon(Zr_3(OH)_9^{3+}, Cl^-)$, are then fitted to the solubility data at $pH_m < 3$ in 0.51, 1.02 and 3.20 m NaCl and in 0.20 and 1.02 m $CaCl_2$:

$$\log^* K°_{s,0} = -4.3 \pm 0.2 \text{ and } \varepsilon(Zr_3(OH)_9^{3+}, Cl^-) = 0.30 \pm 0.11 \text{ kg·mol}^{-1}$$

The corresponding solubility product, $\log K°_{sp} = \log^* K°_{s,0} + 4 \log K°_w = -60.3 \pm 0.2$ (referring to the reaction $Zr(OH)_4(s) \Leftrightarrow Zr^{4+} + 4\, OH^-$), is typical for an aged Zr(IV) oxyhydroxide precipitate, *i.e.*, it is lower than the value selected in the NEA-TDB for fresh $Zr(OH)_4(am)$ precipitates ($\log K°_{sp} = -59.24 \pm 0.10$, $\log^* K°_{s,0} = -3.24 \pm 0.10$ [3]) but greater than the value proposed for monoclinic $ZrO_2(cr)$ ($\log K°_{sp} = -63.0 \pm 1.6$, $\log^* K°_{s,0} = -7.0 \pm 1.6$ [3]). The SIT coefficient $\varepsilon(Zr_3(OH)_9^{3+}, Cl^-) = 0.30 \pm 0.11$ kg·mol^{-1} is in the expected range (0.35 ± 0.17 kg·mol^{-1}) with regard to the value of $\varepsilon(Zr_3(OH)_9^{3+}, ClO_4^-) = 0.93 \pm 0.35$ kg·mol^{-1} [3] and the relation $\varepsilon(M^{z+}, Cl^-) = 0.38\, \varepsilon(M^{z+}, ClO_4^-) \pm 0.1$ kg·mol^{-1} [4, 23].

Model calculations including the NEA-TDB data for the species $Zr_4(OH)_{15}^+$ overestimate the solubility at pH_c around 3 (*c.f.*, fat dashed lines in Figs.2a-c). Neither our data nor the data of Sasaki et al. [6] in 0.1, 0.5 and 1.0 M $NaClO_4$ (for a solid with $\log^* K°_{s,0} = -3.6 \pm 0.3$ where the concentration $[Zr]_{(4,15)}$ is expected to be 2.8 log-units greater than for our solid) show any evidence for contributions from the complex $Zr_4(OH)_{15}^+$; they are much better reproduced if this complex is excluded (fat solid lines in Figs.2a-c), *i.e.*, $\log^* \beta°_{4,15} < 11$. Brown et al. derived the equilibrium constant $\log^* \beta°_{4,15} = 12.6$ from solubility data for fresh $Zr(OH)_4(am)$ precipitates which decrease from about 10^{-1} to 10^{-3} M at pH 1 - 3 (*c.f.*, Appendix D in [3].) The slope of -1 indicates the dominance of a complex with charge z = +1 but not whether it is a tetramer. Possibly larger oligomers dominate as indicated by the results of Walther et al. [22] at similar H^+ and Zr concentrations. At the much lower Zr concentrations in the present study with aged $ZrO_2 \cdot xH_2O(s)$ the corresponding equilibrium concentration of larger oligomers (e.g., of an octamer $Zr_8(OH)_{31}^+$) would be negligibly small.

The pH-independent, constant solubility in the intermediate pH range (pH_c = 3 - 12 in NaCl and 3 - 10 in $CaCl_2$ solutions) is described by the reaction

$$Zr(OH)_4(s) \Leftrightarrow \text{"}Zr(OH)_4(aq)\text{"} \qquad (7)$$

The present results yield an equilibrium constant of log $K_{s,4}$ = log ["$Zr(OH)_4$(aq)"] = - 7.8 ± 0.7. "$Zr(OH)_4$(aq)" stands for neutral species $Zr_m(OH)_{4m}$(aq), either monomers or oligomers with $m < 10$ (*c.f.*, discussion for thorium [4]). The true concentration of mononuclear $Zr(OH)_4$(aq) species is probably much lower. The interaction coefficients of neutral species can usually be set equal to zero. The equilibrium constants selected in the NEA-TDB, $\log^*\beta°_{1,4}$ = - 2.2 ± 1.7 and $\log^*\beta°_{4,16}$ = 8.4 ± 0.8 [3], combined with $\log^*K°_{s,0}$ = - 4.3 ± 0.2, gives log $[Zr]_{(1,4)}$ = - 6.5 ± 1.7 (higher than but within the uncertainty consistent with our data) and log $[Zr]_{(4,16)}$ = - 8.2 ± 1.1 (also in the range of the present results).

3.1.2. Equilibrium constants for Zr(IV) complexes in alkaline solutions

The solubility increase at $pH_c > 13$ in 0.5, 1.0 and 3.0 M NaCl-NaOH and in pure 1.0, 5.0 and 10 M NaOH [5] is consistent with the equilibrium

$$Zr(OH)_4(s) + 2\ OH^- \Leftrightarrow Zr(OH)_6^{2-} \qquad (8)$$

$$\log K_{s,6} = \log [Zr(OH)_6^{2-}] - 2 \log [OH^-]$$
$$= \log K°_{s,6} + 2\ D - \varepsilon(Zr(OH)_6^{2-}, Na^+)\ m_{Na^+} + 2\ \varepsilon(OH^-, Na^+)\ m_{Na^+} \qquad (9)$$

When the term (log $K_{s,6}$ - 2D) is plotted vs. I_m for the extrapolation to I = 0 (Fig. 3a), the experimental log $K_{s,6}$ values in 0.5, 1.0, and 3.0 M NaCl solution lead to log $K°_{s,6}$ = - 5.5 ± 0.2. The slope ($s = -\Delta\varepsilon = -\varepsilon(Zr(OH)_6^{2-}, Na^+) + 2\ \varepsilon(OH^-, Na^+) = 0.10 \pm 0.03$ kg·mol^{-1}) corresponds to $\varepsilon(Zr(OH)_6^{2-}, Na^+) = -0.02 \pm 0.04$ kg·mol^{-1}. The data of Ekberg et al. [5] in 1.0, 5.0 and 10 M NaOH (m_{NaOH} = 1.00, 5.09 and 10.80 mol/kg [24]), lead to a slightly lower value of log $K°_{s,6}$ = - 5.7 ± 0.1 (Fig. 3a). However, the slope ($s = -\Delta\varepsilon = -0.02 \pm 0.01$ kg·mol^{-1}) and hence $\varepsilon(Zr(OH)_6^{2-}, Na^+) = 0.10 \pm 0.02$ kg·mol^{-1} is noticeably different. Since our results in pure 0.5, 1.0 and 3.0 M NaOH are consistent with this $\varepsilon(Zr(OH)_6^{2-}, Na^+)$ value (*c.f.*, Fig. 3a) we assume that the systematic deviation from $\varepsilon(Zr(OH)_6^{2-}, Na^+)$ in NaCl solution is not due to experimental errors but to anion-anion interaction terms neglected in the SIT model (similar examples are discussed in Appendix D of [2]) and propose a mean value of $\varepsilon(Zr(OH)_6^{2-}, Na^+) = 0.04 \pm 0.08$ kg·mol^{-1}.

For the apparent equilibrium constants log $K_{s,4}$ in $CaCl_2$ solution the term (log $K_{s,4}$ - 2 D) does not follow the linear SIT relationship for the extrapolation to I = 0 but shows an exponential decrease at low ionic strength (Fig. 3a). At a given pH, the concentration of $Zr(OH)_6^{2-}$ in 0.2 m $CaCl_2$ (I_m = 0.6 mol·kg^{-1}) is more than 4 orders of magnitude above that in 0.5 m NaCl. Such a large difference at relatively low ionic strength cannot be explained by differences in the ion interaction parameters $\varepsilon(Zr(OH)_6^{2-}, Na^+)$ and $\varepsilon(Zr(OH)_6^{2-}, Ca^{2+})$. It is evident that the experimental data can only be explained by equilibria involving complexes with Ca^{2+} ions:

$$Zr(OH)_4(s) + 2\ OH^- + n\ Ca^{2+} \Leftrightarrow Ca_n[Zr(OH)_6]^{2n-2} \qquad (10)$$

$$\log K_{s,(n,1,6)} = \log [Ca_n[Zr(OH)_6]^{2n-2}] - 2 \log [OH^-] - n \log [Ca^{2+}]$$
$$= \log K°_{s,(n,1,6)} + \Delta z^2 D - \varepsilon(Ca_n[Zr(OH)_6]^{2n-2}, Cl^-)\, m_{Cl^-}$$
$$+ 2\, \varepsilon(OH^-, Ca^{2+})\, m_{Ca^{2+}} + n\, \varepsilon(Ca^{2+}, Cl^-)\, m_{Cl^-} \quad (11)$$

An attempt to describe the experimental data with the assumption that one Ca^{2+} ion (n = 1) is coordinated to $[Zr(OH)_6^{2-}]$ failed and an attempt assuming n = 2 was only successful, if the data at the two highest $CaCl_2$ concentrations were excluded. The corresponding SIT regression plots of $\log K_{s,(n,1,6)} - \Delta z^2 D$ vs. I_m do not show a linear relationship. The calculation for n = 3 (in agreement with $N_{Ca} = 2.7 \pm 0.6$ determined by EXAFS [14]):

$$Zr(OH)_4(s) + 2\, OH^- + 3\, Ca^{2+} \Leftrightarrow Ca_3[Zr(OH)_6]^{4+} \quad (12)$$

yields $\log K°_{s,(3,1,6)} = 0.7 \pm 0.3$ and $\varepsilon(Ca_3[Zr(OH)_6]^{4+}, Cl^-) = 0.48 \pm 0.10$ kg·mol^{-1} (Fig.3b) and describes the experimental data at all $CaCl_2$ concentrations reasonably well (dashed lines in Fig. 4). A slightly better fit (solid lines in Fig. 4) is obtained if the number of associated Ca^{2+} ions is assumed to vary with the $CaCl_2$ concentration, *i.e.*, by including both $Ca_3[Zr(OH)_6]^{4+}$ (dominant at $CaCl_2$ > 0.2 M) and $Ca_2[Zr(OH)_6]^{2+}$ (dominant at $CaCl_2$ < 0.2 M):

$$\log K°_{s,(3,1,6)} = 0.5 \pm 0.2 \text{ and } \varepsilon(Ca_3[Zr(OH)_6]^{4+}, Cl^-) = 0.40 \pm 0.07 \text{ kg·mol}^{-1}$$
$$\log K°_{s,(2,1,6)} = 1.1 \pm 0.2 \text{ and } \varepsilon(Ca_2[Zr(OH)_6]^{2+}, Cl^-) = 0.1 \pm 0.1 \text{ kg·mol}^{-1}$$

With $\log K°_{sp} = -60.3 \pm 0.2$ the complex formation constants $\log \beta°_{n,1,6}$ for the reactions

$$Zr^{4+} + 6\, OH^- + n\, Ca^{2+} \Leftrightarrow Ca_n[Zr(OH)_6]^{2n-2} \quad (13)$$

are $\log \beta°_{0,1,6} = 54.8 \pm 0.3$ (NEA-TDB [3]: 55.0 ± 0.7), $\log \beta°_{2,1,6} = 61.4 \pm 0.3$ and $\log \beta°_{3,1,6} = 60.8 \pm 0.3$. The complex $Ca[Zr(OH)_6](aq)$ does not play any role at $[Ca^{2+}]$ > 0.1 M. However, assuming a linear decrease of $\log K°_n$ for the stepwise association of Ca^{2+} ions to $Zr(OH)_6^{2-}$ ($Ca_{n-1}[Zr(OH)_6]^{2n-4-} + Ca^{2+} \Leftrightarrow Ca_n[Zr(OH)_6]^{2n-2}$, with $\log K°_1 = 4.6$, $\log K°_2 = 2.0$, $\log K°_3 = -0.6$) we estimate: $\log \beta°_{1,1,6} = 59.4 \pm 0.3$.

3.2. Solubility of Th(IV) hydrous oxide in alkaline $CaCl_2$ solutions

The solubility of Th(IV) hydrous oxide in sodium, lithium and tetramethylammonium hydroxide solutions shows no increase up to pH 14, no indication for the formation of anionic Th(IV) hydroxide complexes with 5 or 6 OH^- ligands at high pH [25]. Solubility data determined after 1.5 - 2 nm ultrafiltration or ultracentrifugation in neutral and alkaline NaCl and $NaClO_4$ media [7, 25-27] are at a constant level of $\log [Th] = \log K_{s,4} = -8.5 \pm 0.6$ [1,7] (Fig. 5). This concentration is due to neutral species $Th_m(OH)_{4m}(aq)$, either monomers or oligomers with m < 10 [4]. Our data in 0.2 M $CaCl_2$ and those at higher $CaCl_2$ concentrations and pH_c < 11 are also in this range. However, the thorium concentrations measured after 7 - 198 days in 0.5, 1.0, 2.0, and 4.5 M $CaCl_2$ in the range pH_c = 11 - 12 show an extremely steep increase and a systematic dependence on the $CaCl_2$ concentration. The observed dependence

on pH_c (slope 4 for log [Th] vs. pH_c) indicates the formation of a Th(IV) hydroxide complex with 8 OH^- ligands which is a very unexpected result. The thorium concentrations measured for comparison after 14 and 27 days in a few samples in 2.0 M $Ca(ClO_4)_2$ (Fig. 5) show the same tendency. Analogous to the behaviour of Zr(IV), the $Th(OH)_8^{4-}$ complex must be stabilized by association of Ca^{2+} ions.

This conclusion was confirmed by an EXAFS spectrum of the solution with the highest Th(IV) concentration ($4.3 \cdot 10^{-3}$ M at pH_c = 12.2 in 4.5 M $CaCl_2$) [14]. This sample was prepared particularly for EXAFS analysis and equilibrated only for one day, because the matrix solution is metastable with regard to the high pH value. The matrix solution was prepared by equilibration of a 4.5 M $CaCl_2$ with $Ca(OH)_2$(cr) for 2 hours; it was removed from the solid phase before $Ca(OH)_2$(cr) started to transform into less soluble calcium hydroxychlorides which leads to a decrease of pH. Longer equilibration of the matrix solution led to pH_c = 11.8 (*c.f.*, Fig. 1) where the solubility of $ThO_2 \cdot xH_2O$(s) is about 1.6 log-units lower (*c.f.*, Fig. 5) and not sufficient for EXAFS analysis. An EXAFS spectrum of the $4.3 \cdot 10^{-3}$ M Th(IV) solution at pH_c = 12.2 in 4.5 M $CaCl_2$ clearly shows a second coordination shell coming from calcium backscatter atoms. The presence of both polynuclear Th(IV) species and chloride ligands can be ruled out. The coordination numbers (N_O = 8.6 ± 1.2, N_{Ca} = 3.8 ± 0.5) and distances ($R_{Th\text{-}O}$ = 2.47 ± 0.03 Å, $R_{Th\text{-}Ca}$ = 3.98 ± 0.02 Å) indicate that four Ca^{2+} ions are bound to the edges of a distorted $Th(OH)_8^{4-}$ polyhedron which possibly includes one or two additional H_2O ligands [14].

These results show that the solubility of $ThO_2 \cdot xH_2O$(am), designated here as $Th(OH)_4$(s), increases in alkaline $CaCl_2$ solutions according to the reaction

$$Th(OH)_4(s) + 4\ OH^- + 4\ Ca^{2+} \Leftrightarrow Ca_4[Th(OH)_8]^{4+} \tag{14}$$

$$\begin{aligned} \log K_{s,(4,1,8)} &= \log [Ca_4[Th(OH)_8]^{4+}] - 4 \log [OH^-] - 4 \log [Ca^{2+}] \\ &= \log K°_{s,(4,1,8)} + \Delta z^2 D - \varepsilon(Ca_4[Th(OH)_8]^{4+}, Cl^-)\ m_{Cl^-} \\ &\quad + 4\ \varepsilon(OH^-, Ca^{2+})\ m_{Ca^{2+}} + 4\ \varepsilon(Ca^{2+}, Cl^-)\ m_{Cl^-} \end{aligned} \tag{15}$$

The corresponding SIT regression plot of ($\log K_{s,(4,1,8)}$ + 4D) vs. I_m (Fig. 6) yields

$$\log K°_{s,(4,1,8)} = 1.8 \pm 0.5 \text{ and } \varepsilon(Ca_4[Th(OH)_8]^{4+}, Cl^-) = -0.01 \pm 0.10\ kg \cdot mol^{-1}.$$

This "two-parameter-fit" describes the measured thorium concentrations very well (*c.f.*, solid lines in Fig. 5) and, contrary to the data for Zr(IV), it is not possible to improve the fit by including complexes $Ca_n[Th(OH)_8]^{4-2n}$ with less than four Ca^{2+} ions. However, the calculated equilibrium constant at I = 0 and particularly the value of $\varepsilon(Ca_4[Th(OH)_8]^{4+}, Cl^-)$ depend strongly on the data in 4.5 M (5.26 m) $CaCl_2$, *i.e.*, at I_m = 15.8 $mol \cdot kg^{-1}$ which is far above the validity range of the SIT. Combined with $\log K°_{s,(4,1,8)}$ = 1.8 ± 0.5 the data in 2.0 M (2.40 m) $Ca(ClO_4)_2$ give a value of $\varepsilon(Ca_4[Th(OH)_8]^{4+}, ClO_4^-)$ = 0.21 ± 0.17 $kg \cdot mol^{-1}$.

Remarks on the solubility limiting solid phase: The hydrous Th(IV) oxide used in the present solubility study was x-ray amorphous as described previously [7, 20]. However, after 6 months in 1.0 - 4.5 M $CaCl_2$ at pH_c > 11.5 several samples of Th(IV) solids show an XRD pattern that could not yet be identified. It is clearly different from that of ThO_2(cr), possibly due to a very slow transformation into a calcium thorate solid. Scanning electron microscopy (SEM) showed needle-like crystals lying on the bulk heap of amorphous $ThO_2 \cdot xH_2O$(am) particles. These indications for a possible solid transformation deserve further investigations. On the other hand, the SEM images also showed that only a part of the $ThO_2 \cdot xH_2O$(am) was transformed. A complete transformation into a more stable solid would cause a noticeable decrease of the solubility with time and also a different dependence on pH. However, this was not observed; the thorium concentrations measured after a few days were not markedly different from those measured after 3 - 6 months, indicating that the initial $ThO_2 \cdot xH_2O$(am) was the solubility controlling solid phase throughout the study.

3.3. Solubility of Pu(IV) hydrous oxide (PuO_{2+x}(am,hyd)) in alkaline $CaCl_2$ solutions

As plutonium is the most hazardous among the actinides, we also investigated the possible solubility increasing effect of ternary Ca-Pu(IV)-OH complexes. For this purpose we continued our recent solubility study with PuO_{2+x}(am,hyd) that contained about 0.5 % of oxidized Pu [16]. The aqueous phase of previous samples (stored in an Ar glove box) was replaced by alkaline $CaCl_2$ matrix solutions. The Pu concentrations measured after 7 - 132 days are shown in Fig. 7 in comparison with previous results in 0.1 M NaCl and similar studies in $NaClO_4$ and dilute KOH solutions, either under Ar [8, 16, 28] or under air [29-31]. Under these conditions the total Pu concentration measured after 1.5 - 2 nm ultrafiltration is dominated by Pu(V) species; a detailed discussion is given in [16]). The Pu(IV) concentration in near-neutral and alkaline solutions is very low and at a constant concentration level of log [Pu(IV)] = - 10.4 ± 0.5 [1, 8]).

The solubility in 1.0 M $CaCl_2$ is in the range of the data in NaCl and $NaClO_4$ media, but at pH_c = 11 - 12 in 2.0 and 4.0 M $CaCl_2$ the measured Pu concentrations increase up to 10^{-8} and 10^{-7} M, respectively. These low concentrations do not allow a reliable oxidation state analysis of the dissolved Pu species, neither by spectroscopy nor (with regard to the detection limits of the Pu-242 used) by solvent extraction methods which require dilution and acidification of the alkaline $CaCl_2$ solution. However, as the tetravalent actinides usually show an analogous chemical behaviour, we assume that the observed solubility increase in $CaCl_2$ solutions is probably caused by a species analogous to the ternary Th(IV) complex:

$$Pu(OH)_4(s) + 4\ OH^- + 4\ Ca^{2+} \Leftrightarrow Ca_4[Pu(OH)_8]^{4+} \qquad (16)$$

With $\log K°_{s,(4,1,8)}$ = - 2.0 ± 0.5 and the same SIT coefficients as for the thorium complex, $\varepsilon(Ca_4[Pu(OH)_8]^{4+}, Cl^-)$ = - 0.01 ± 0.10 $kg \cdot mol^{-1}$, the experimental Pu concentrations are well

described (*c.f.*, Fig. 7 where the calculated $Ca_4[Pu(OH)_8]^{4+}$ concentrations are shown as thin solid lines). This equilibrium constant is 3.8 log-units smaller than for Th(IV), but with the known solubility products of the hydrous oxides, $\log K°_{sp} = -47.8 \pm 0.3$ for Th(IV) [7] and -58.3 ± 0.5 for Pu(IV) [2], the complex formation constants (referring to the reaction $An^{4+} + 8\ OH^- + 4\ Ca^{2+} \Leftrightarrow Ca_4[An(OH)_8]^{4+}$) are $\log \beta°_{4,1,8} = 49.6 \pm 0.6$ for Th(IV) and 56.3 ± 0.7 for Pu(IV). They show the expected tendency in the actinide series where the formation constants of aqueous complexes generally increase from Th(IV) to Pu(IV).

The redox conditions in the investigated $CaCl_2$ solutions are similar to those in our previous study in 0.1 M NaCl [16]: $E_h = 0.1$ to 0.3 V at $pH_c = 11 - 12$, (pe + pH) = 14 ± 2. Under these conditions aqueous Pu(III) species do not play any role. However, as the solid phase is in equilibrium with both Pu(IV) and Pu(V) species, we cannot rule out possible effects from ternary Ca-Pu(V)-OH or Ca-Pu(VI)-OH complexes like $Ca_2[PuO_2(OH)_4]^{z+}$ or $Ca_3[PuO_2(OH)_6]^{z+}$ which might also stabilized in alkaline $CaCl_2$ solutions. This is not yet known. Therefore, the interpretation suggested by the analogy to the Th(IV) data requires confirmation under more reducing conditions where the interference of Pu(V) and Pu(VI) species can be excluded. At present it has to be considered as an upper limit for the solubility increasing effect of ternary Ca-Pu(IV)-OH complexes.

4. Conclusions

In alkaline $CaCl_2$ and $Ca(ClO_4)_2$ solutions the solubility of the oxides/hydroxides of tetravalent metal ions is significantly increased by the formation of ternary Ca-M(IV)-OH complexes with unusually high numbers of hydroxide ligands. Thermodynamic data for these complexes are derived with the SIT. At the Migration '07 conference comparable results were presented for trivalent lanthanides and actinides; the solubility of $Nd(OH)_3(s)$ and a fluorescence emission spectra of Cm(III) provide strong evidence for the formation of ternary Ca-M(III)-OH complexes in alkaline 1.0 - 3.5 M $CaCl_2$ solutions [32, 33]. A similar type of ternary complexes, calcium-uranyl(VI)-carbonate complexes, $Ca[UO_2(CO_3)_3]^{2-}$ and $Ca_2[UO_2(CO_3)_3]°$, has been observed in $NaClO_4$ solutions [34 - 36], at low Ca^{2+} concentrations (10^{-3} to 10^{-2} M) limited by the solubility of calcite. The stabilization of anionic hydroxide and carbonate complexes by Ca^{2+} ions seems to be a general phenomenon that can have a significant impact on the solubility and aqueous speciation of actinides, particularly in aqueous systems with cementitious waste forms.

It may appear somewhat strange that complexes like $Ca_3[Zr(OH)_6]^{4+}$ and $Ca_4[Th(OH)_8]^{4+}$ with a high nominal positive charge exist in alkaline solutions without charge compensation by association of further anions. However, one has to take into account that the charge distribution in these ternary Ca-M-OH complexes is not comparable with that in metal ions M^{z+} of the same nominal charge. The charge of $M^{z+}(aq)$ ions is usually compensated by hydrolysis reactions, but the central metal ion in the ternary Ca-M(IV)-OH complexes is

already completely hydrolysed, its charge is even overcompensated and no further Cl^- ligands are added as shown by EXAFS [14]. There is no high local positive charge in the ternary complexes $Ca_3[Zr(OH)_6]^{4+}$ and $Ca_4[Th(OH)_8]^{4+}$. The central complexes $[Zr(OH)_6^{2-}]$ and $[Th(OH)_8^{4-}]$ have a negative charge and the total nominal charge of +4 is distributed to the 3 or 4 surrounding calcium ions. As these Ca^{2+} ions are directly associated to two OH^- ligands of the central hydroxide complex, their charge is already partly compensated; hence their tendency to form ion pairs with medium anions is even smaller than for Ca^{2+} ions of the bulk medium. Because of the considerably different charge distribution in the ternary Ca-M(IV)-OH compared to metal ions M^{z+}, it is also to note that the corresponding ion interaction (SIT) coefficients are not necessarily similar.

References

1. Neck, V., Kim, J.I., Solubility and hydrolysis of tetravalent actinides. Radiochim. Acta **89**, 1-16 (2001).

2. Guillaumont, R., Fanghänel, Th., Fuger, J., Grenthe, I., Neck, V., Palmer, D.A., Rand, M.H. (OECD, NEA-TDB). Chemical Thermodynamics Vol. 5. Update on the Chemical Thermodynamics of Uranium, Neptunium, Plutonium, Americium and Technetium. Elsevier, Amsterdam (2003).

3. Brown, P.L., Curti, E., Grambow, B., Ekberg, C. (OECD, NEA-TDB). Chemical Thermodynamics Vol. 8. Chemical Thermodynamics of Zirconium. Elsevier, Amsterdam (2005).

4. Rand, M.H., Fuger, J., Grenthe, I., Neck, V. Rai, D.: Chemical Thermodynamics Vol.11, Chemical Thermodynamics of Thorium. OECD Nuclear Energy Agency (Eds.: F. Mompean, M. Illemassene, J. Perrone), in print.

5. Ekberg, C., Källvenius, G., Albinsson, Y., Brown, P.L.: Studies on the Hydrolytic Behavior of Zirconium(IV). J. Solution Chem. **33**, 47-79 (2004).

6. Sasaki, T., Kobayashi, T., Tagaki, I., Moriyama, H.: Solubility measurement of zirconium(IV) hydrous oxide. Radiochim. Acta **94**, 489-494 (2006).

7. Neck, V., Müller, R., Bouby, M., Altmaier, M., Rothe J., Denecke, M.A., Kim, J.I.: Solubility of amorphous Th(IV) hydroxide - application of LIBD to determine the solubility product and EXAFS for aqueous speciation. Radiochim. Acta **90**, 485 - 494 (2002).

8. Rai, D., Hess, N.J., Felmy, A.R., Moore, D.A., Yui, M., Vitorge, P.: A Thermodynamic Model for the Solubility of PuO_2(am) in the Aqueous K^+-HCO_3^--CO_3^{2-}-OH^--H_2O System; Radiochim. Acta **86**, 89-99 (1999).

9. Fujiwara, K., Yamana, H., Fujii, T., Kawamoto, K., Sasaki, T., Moriyama, H.: Solubility of uranium(IV) hydrous oxide in high pH solution under reducing condition. Radiochim. Acta **93**, 347-350 (2005).

10. Gayer, K.M., Leider, H.: The solubility of uranium(IV) hydrous oxide in solutions of sodium hydroxide and perchloric acid under reducing condition at 25°C. Can. J. Chem. **35**, 5-7 (1957).

11. Peretrukhin, V.F., Kryutchkov, S.V., Silin, V.I., Tananaev, I.G.: Determination of the Solubility of Np(IV)-(VI). Pu(III)-(VI), Am(III)-(VI) and Tc(IV), (V) Hydroxo Compounds in 0.5 - 14 M NaOH Solutions. Report WHC-EP-0987, Westinghouse Hanford Company, Richland, Washington, 1996.

12. Sheka, I.A., Pevzner, T.V.: Solubility of zirconium and hafnium hydroxides in sodium hydroxide solutions. Russ. J. Inorg. Chem.. **5**, 1119-1121 (1960).

13. Adair, J.H., Denkewicz, R.P., Arriagada, F.J., Osseo-Assare, K.: Precipitation and in-situ transformation in the hydrothermal synthesis of crystalline zirconium dioxide. Ceramic Trans. **1**, 135-145 (1987).

14. Brendebach, B., Altmaier, M., Rothe, J., Neck, V., Denecke, M.A.: EXAFS Study of Aqueous Zr^{IV} and Th^{IV} Complexes in Alkaline $CaCl_2$ Solutions: $Ca_3[Zr(OH)_6]^{4+}$ and $Ca_4[Th(OH)_8]^{4+}$. Inorg. Chem. **46**, 6804 - 6810 (2007).

15. Harvie, C. F., Møller, N., Weare, J.H., The prediction of mineral solubilities in natural waters: The Na-K-Mg-Ca-H-Cl-SO_4-OH-HCO_3-CO_2-H_2O system to high ionic strengths at 25°C. Geochim. Cosmochim. Acta **48**, 723-751 (1984).

16. Neck, V., Altmaier, M., Seibert, A., Yun, J.I., Marquardt, C.M., Fanghänel, Th.: Solubility and redox reactions of Pu(IV) hydrous oxide: Evidence for the formation of PuO_{2+x}(s, hyd). Radiochim. Acta **95**, 193-207 (2007).

17. Altmaier, M., Metz, V., Neck, V., Müller, R., Fanghänel, Th.: Solid-liquid equilibria of $Mg(OH)_2$(cr) and $Mg_2(OH)_3Cl \cdot 4H_2O$(cr) in the system Mg-Na-H-OH-Cl-H_2O at 25°C. Geochim. Cosmochim. Acta **67**, 3595 - 3601 (2003).

18. Baes, C.F.,Jr., Mesmer, R.E.: The Hydrolysis of Cations. Wiley, New York, 1976.

19. Cho, H.R., Walther, C., Rothe, J., Neck, V., Denecke, M.A., Dardenne, K., Fanghänel, Th.: Combined LIBD and XAFS Investigation of the Formation and Structure of Zr(IV) Colloids. Anal. Bioanal. Chem. **383**, 28 - 40 (2005).

20. Neck, V., Altmaier, M., Müller, R., Bauer, A., Fanghänel, Th., Kim, J.I.: Solubility of crystalline thorium dioxide. Radiochim. Acta 91, 253 - 262 (2003).

21. Rai, D., Yui, M., Moore, D.A.: Solubility and Solubility Product at 22°C of UO_2(c) Precipitated From Aqueous U(IV) Solutions. J. Solution Chem. **32**, 1-17 (2003).

22. Walther, C., Rothe, J., Fuss, M., Büchner, S., Koltsov, S., Bergmann, T.: Investigation of polynuclear Zr(IV) hydroxide complexes by nanoelectrospray mass-spectrometry combined with XAFS. Anal. Bioanal. Chem. **388**, 409 - 431 (2007).

23. Neck, V., Altmaier, M., Fanghänel, Th.: Ion interaction (SIT) coefficients for the Th^{4+} ion and trace activity coefficients in $NaClO_4$, $NaNO_3$ and NaCl solution determined by solvent extraction with TBP. Radiochim. Acta **94**, 501-507 (2006).

24. Marcus, Y., Kertes, A.S.: Ion exchange and solvent extraction of metal complexes. Wiley, London, New York, 1969.

25. Ryan, J.L., Rai, D.: Thorium(IV) Hydrous Oxide Solubility. Inorg. Chem. **26**, 4140-4142 (1987).

26. Moon, H.C.: Equilibrium Ultrafiltration of Hydrolized Thorium(IV) Solutions. Bull. Korean Chem. Soc. **10**, 270-272 (1989).

27. Felmy, A.R., Rai, D., Mason, M.J.: The Solubility of Hydrous Thorium(IV) Oxide in Chloride Media: Development of an Aqueous Ion-Interaction Model; Radiochim. Acta **55**, 177-185 (1991).

28. Lierse, Ch., Kim, J.I.: Chemisches Verhalten von Plutonium in natürlichen aquatischen Systemen: Hydrolyse, Carbonatkomplexierung und Redoxreaktionen. Report RCM 02286, Inst. für Radiochemie, Technische Universität München (1986).

29. Rai, D., Serne, R.J., Moore, D.A.: Solubility of Plutonium Compounds and Their Behavior in Soils. Soil Sci. Am. J. **44**, 490-495 (1980).

30. Rai, D.: Solubility Product of Pu(IV) Hydrous Oxide and Equilibrium Constants of Pu(IV)/Pu(V), Pu(IV)/Pu(VI), and Pu(V)/Pu(VI) Couples. Radiochim. Acta **35**, 97-106 (1984).

31. Rai, D., Moore, D.A., Felmy, A.R., Choppin, G.R., Moore, R.C., Thermodynamics of the PuO_2^+-Na^+-OH^--Cl^--ClO_4^--H_2O system: use of NpO_2^+ Pitzer parameters for PuO_2^+. Radiochim. Acta **89**, 491-498 (2001).

32. Neck, V., Altmaier, M., Lützenkirchen, J., Korthaus, E., Fanghänel, Th.: A comprehensive thermodynamic model for the solubility and hydrolysis of Nd(III) and Am(III) in dilute to concentrated NaCl, $MgCl_2$ and $CaCl_2$ solutions. Presented at the conference Migration '07, to be published.

33. Rabung, Th., Altmaier, M., Neck, V., Fanghänel, Th.: A TRLFS study of Cm(III) hydroxide complexes in alkaline $CaCl_2$ solution. Presented at the conference Migration '07, to be published.

34. Bernhard, G., Geipel, G., Brendler, V., Nitsche, H.: Speciation of uranium in seepage waters of a mine tailing pile studied by time-resolved laser-induced fluorescence spectroscopy (TRLFS). Radiochim. Acta **74**, 87-91 (1996).

35. Bernhard, G., Geipel, G., Reich, T., Brendler, V., Amayri, S., Nitsche, H.: Uranyl(VI) carbonate complex formation: Validation of the $Ca_2UO_2(CO_3)_3$(aq) species. Radiochim. Acta **89**, 511-518 (2001).

36. Kalmykov, S.N., Choppin, G.R.: Mixed $Ca^{2+}/UO_2^{2+}/CO_3^{2-}$ complex formation at different ionic strengths. Radiochim. Acta **88**, 603-606 (2000).

Table 1. Standard state equilibrium constants (I = 0, 25°C) used in the present calculations of the solubility and hydrolysis of Zr(IV), either adopted from the NEA-TDB [3] or evaluated in the present work (p.w.)

$Zr(OH)_4(s)$ (or $ZrO_2(s) + 2\ H_2O$) + 4 $H^+ \Leftrightarrow Zr^{4+} + 4H_2O$		
$Zr(OH)_4$(am, fresh)	$\log{*}K°_{s,0}$	- 3.2 ± 0.1
$ZrO_2 \cdot xH_2O$(aged)	$\log{*}K°_{s,0}$	- 3.6 to -5.0
		- 4.3 ± 0.2 (p.w.)
ZrO_2(cr)	$\log{*}K°_{s,0}$	- 7.0 ± 1.7
$m\ Zr^{4+} + n\ H_2O \Leftrightarrow Zr_m(OH)_m^{4m-n} + n\ H^+$		
$Zr(OH)^{3+}$	$\log{*}\beta°_{1,1}$	0.32 ± 0.22 [a)]
$Zr(OH)_2^{2+}$	$\log{*}\beta°_{1,2}$	0.98 ± 1.06 [a)]
$Zr(OH)_4$(aq)	$\log{*}\beta°_{1,4}$	(- 2.2 ± 1.7) [b)]
$Zr(OH)_6^{2-}$	$\log{*}\beta°_{1,6}$	(- 29.0 ± 0.7) / - 29.2 ± 0.3 (p.w.)
$Zr_3(OH)_4^{8+}$	$\log{*}\beta°_{3,4}$	0.4 ± 0.3 [a)]
$Zr_3(OH)_9^{3+}$	$\log{*}\beta°_{3,9}$	12.19 ± 0.08
$Zr_4(OH)_8^{8+}$	$\log{*}\beta°_{4,8}$	6.52 ± 0.65 [a)]
$Zr_4(OH)_{15}^{+}$	$\log{*}\beta°_{4,15}$	(12.58 ± 0.24) / < 11 [a)] (p.w.)
$Zr_4(OH)_{16}$(aq)	$\log{*}\beta°_{m,n}$	(8.39 ± 0.80) [b)]
$Zr^{4+} + 6\ OH^- + n\ Ca^{2+} \Leftrightarrow Ca_n[Zr(OH)_6]^{2n-2}$		
$Zr(OH)_6^{2-}$	$\log \beta°_{0,1,6}$	54.8 ± 0.3 (p.w.)
$Ca[Zr(OH)_6]$(aq)	$\log \beta°_{1,1,6}$	(59.4 ± 0.3) [a, c)] (p.w.)
$Ca_2[Zr(OH)_6]^{2+}$	$\log \beta°_{2,1,6}$	61.4 ± 0.3 (p.w.)
$Ca_3[Zr(OH)_6]^{4+}$	$\log \beta°_{3,1,6}$	60.8 ± 0.3 (p.w.)

a) Not relevant under the experimental conditions of the present study.

b) Not used in the present work; for reasons discussed in the text, the constant solubility of different Zr(IV) oxides / hydroxides in neutral solutions is better reproduced by: $\log [Zr]_{(m,4m)} = \log K°_{s,4} = -7.8 \pm 0.7$ for the reaction $Zr(OH)_4(s) \Leftrightarrow$ "$Zr(OH)_4$(aq)".

c) Estimated, see text.

Table 2. Ion interaction (SIT) coefficients ε_{ij} (kg·mol^{-1}) used for the present calculations (from NEA-TDB [2,3], except otherwise stated)

i	j = ClO_4^-	j = Cl^-
H^+	0.14 ± 0.02	0.12 ± 0.01
Ca^{2+}	0.27 ± 0.03	0.14 ± 0.01
Zr^{4+}	0.89 ± 0.10	0.33 ± 0.09
$Zr(OH)^{3+}$	0.57 ± 0.13	0.22 ± 0.11 [a)]
$Zr(OH)_2^{2+}$	0.62 ± 0.39	0.24 ± 0.18 [a)]
$Zr_3(OH)_4^{8+}$	1.89 ± 0.31	0.33 ± 0.28 [a)]
$Zr_3(OH)_9^{3+}$	0.93 ± 0.35	0.30 ± 0.11 [b)] (p.w.)
$Zr_4(OH)_8^{8+}$	3.61 ± 1.02	1.37 ± 0.40 [a)]
$Zr_4(OH)_{15}^{+}$	0.09 ± 0.92	0.03 ± 0.36 [a)]
$Zr(OH)_4$(aq)	0	0
$Zr_4(OH)_{16}$(aq)	0	0
$Ca[Zr(OH)_6]$(aq)	0 [c)]	0 [c)]
$Ca_2[Zr(OH)_6]^{2+}$	0.3 ± 0.1 [c)]	0.1 ± 0.1 [c)] (p.w.)
$Ca_3[Zr(OH)_6]^{4+}$	0.89 ± 0.12 [b)]	0.40 ± 0.07 [b)] (p.w.)
$Ca_4[Th(OH)_8]^{4+}$	0.21 ± 0.17 [b)]	-0.01 ± 0.10 [b)] (p.w.)

i	j = Na^+	j = Ca^{2+}
OH^-	0.04 ± 0.01	- 0.45 ± 0.03 [d)] (p.w.)
$Zr(OH)_6^{2-}$	0.04 ± 0.08 [b,e)] (p.w.)	0 [f)] (p.w.)
$Zr(OH)_4$(aq)	0	0 [c)]
$Zr_4(OH)_{16}$(aq)	0	0 [c)]
$Ca[Zr(OH)_6]$(aq)	0 [c)]	0 [c)]

[a)] Estimated according to the correlation: $\varepsilon(M^{z+}, Cl^-) = 0.38\ \varepsilon(M^{z+}, ClO_4^-) \pm 0.1$ kg·mol^{-1}, valid for metal ions M^{z+} with z = 1-4 and complexes $Th_m(OH)_n^{z+}$ with z = 0-10 [4, 23].

[b)] Determined from experimental data in NaCl, $CaCl_2$ and $Ca(ClO_4)_2$ solutions (p.w.)

[c)] Estimated by analogy from known SIT coefficients for ions with the same charge.

[d)] Derived from log γ_{OH^-} in 0 - 5 m $CaCl_2$ solution; based on the widely accepted set of Pitzer parameters reported by Harvie et al. [15].

[e)] Mean value from the values of $\varepsilon(Zr(OH)_6^{2-}, Na^+) = -0.02 \pm 0.04$ and 0.10 ± 0.02 kg·mol^{-1} in NaCl and NaOH solutions, respectively (see text). The NEA-TDB review [3] proposed an estimate of $\varepsilon(Zr(OH)_6^{2-}, Na^+) = -0.1 \pm 0.1$ kg·mol^{-1}.

[f)] Interactions must be expressed in terms of complex formation with Ca^{2+} ions.

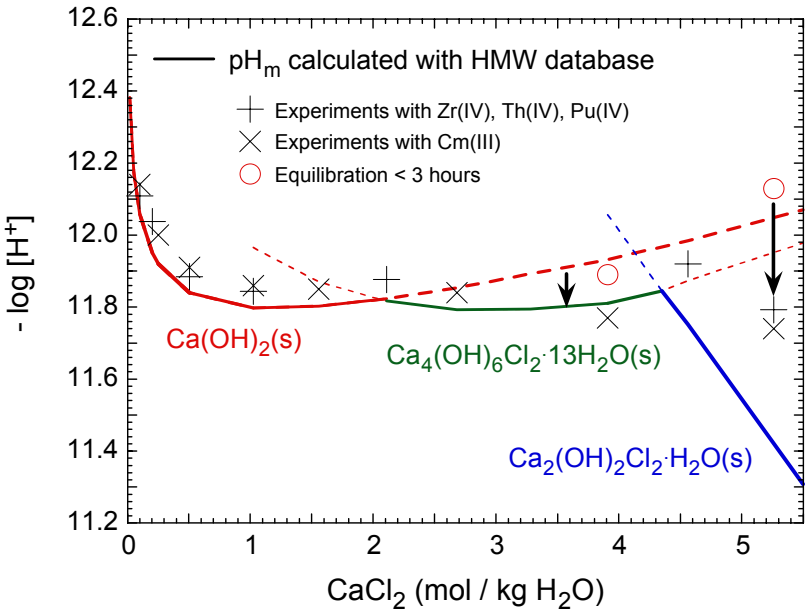

Fig. 1. Experimental pH_m values in $CaCl_2$ matrix solutions equilibrated for about one week (circles: 2 - 3 hours) with calcium hydroxide and/or hydroxychlorides; equilibrium pH_m values calculated with the thermodynamic data and parameters of Harvie et al. [15] are shown as solid lines.

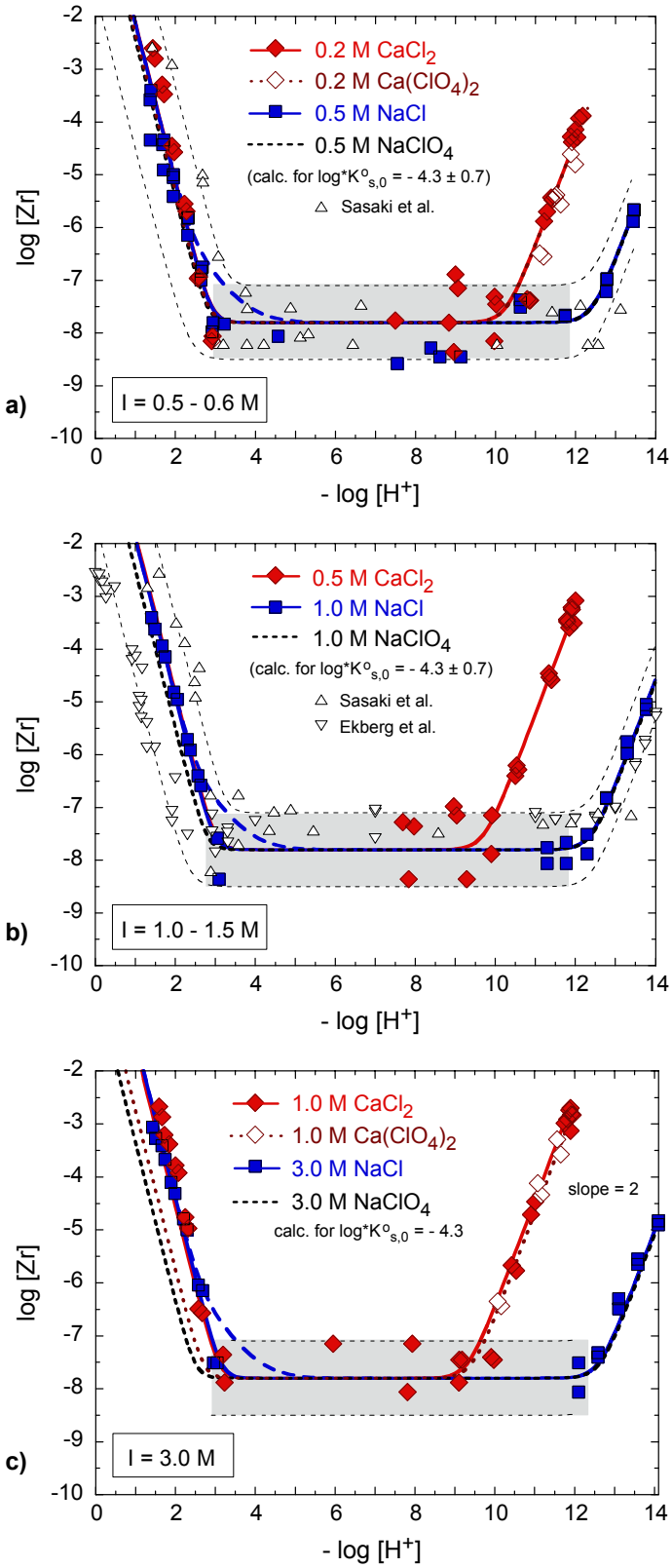

Fig. 2. Solubility of $ZrO_2 \cdot xH_2O(s)$ in NaCl, $NaClO_4$ (data from [5,6]), $CaCl_2$ and $Ca(ClO_4)_2$ solutions of comparable ionic strength: a) I = 0.5 - 0.6 M, b) I = 1.0 - 1.5 M, and c) I = 3.0 M. The fat lines (solid lines for NaCl and $CaCl_2$, dashed lines for $NaClO_4$ and dotted lines for $Ca(ClO_4)_2$ solutions) are calculated for $\log^*K^\circ_{s,0}$ = - 4.3 with the equilibrium constants and SIT coefficients in Tables 1 and 2. The upper and lower thin dashed lines refer to $NaClO_4$ solutions and solids with $\log^*K^\circ_{s,0}$ = - 3.7 and - 5.0, respectively.

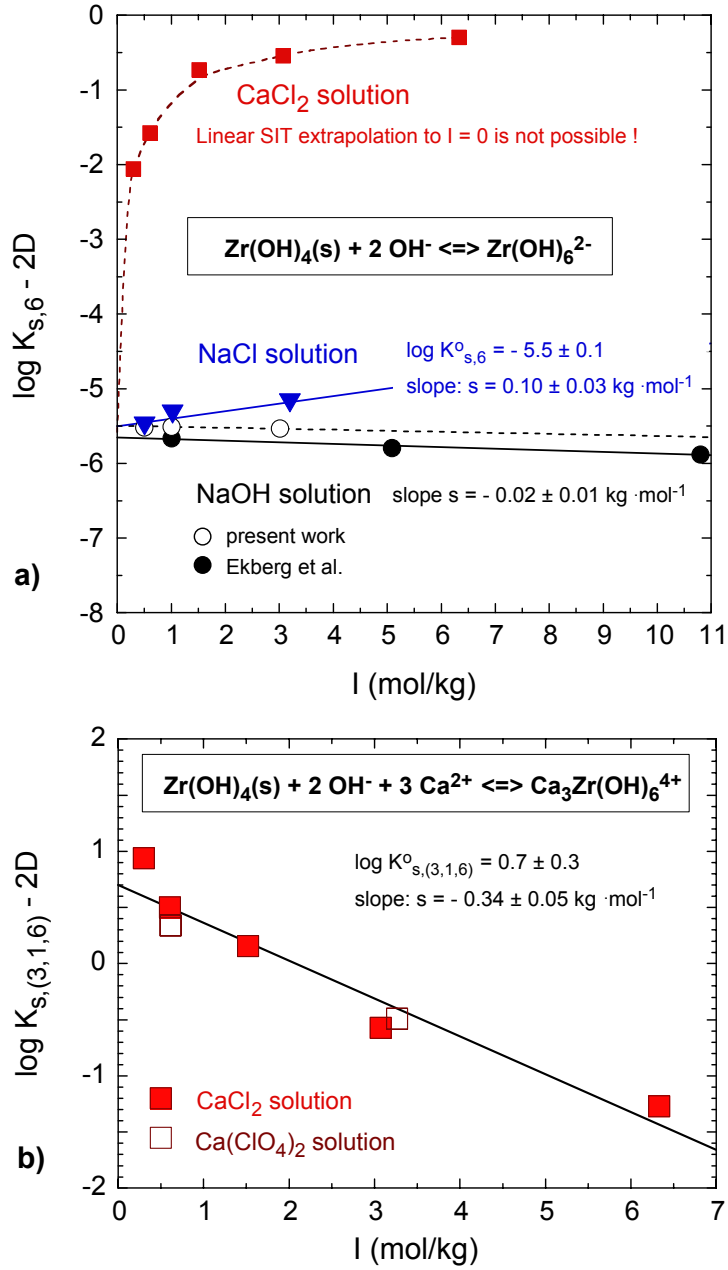

Fig. 3. Application of the linear SIT regression to evaluate the equilibrium constant at I = 0.

a) Reaction: $Zr(OH)_4(s) + 2\ OH^- \Leftrightarrow Zr(OH)_6^{2-}$. The slope s in the plot of (log $K_{s,6}$ - 2D) vs I_m, s = 0.10 ± 0.03 kg·mol^{-1} for data in NaCl and - 0.02 ± 0.01 kg·mol^{-1} for data in pure NaOH solutions (conversion factors m_{NaOH}/c_{NaOH} are taken from [24]), is related to the individual SIT coefficients by: $s = -\Delta\varepsilon = -\varepsilon(Zr(OH)_6^{2-}, Na^+) + 2\ \varepsilon(OH^-, Na^+)$.

b) Reaction: $Zr(OH)_4(s) + 3\ Ca^{2+} + 2\ OH^- \Leftrightarrow Ca_3[Zr(OH)_6]^{4+}$ in $CaCl_2$ solutions.
Since $m_{Ca2+} = m_{CaCl2} = (1/3)\ I_m$ and $m_{Cl-} = 2\ m_{CaCl2} = (2/3)\ I_m$ the slope s = - 0.34 ± 0.05 kg·mol^{-1} in the plot of (log $K_{s,(3,1,6)}$ - 2D) vs I_m is related to the individual SIT coefficients by:
$s = -(2/3)\ \varepsilon(Ca_3[Zr(OH)_6]^{4+}, Cl^-) + 2 \times (1/3)\ \varepsilon(OH^-, Ca^{2+}) + 3 \times (2/3)\ \varepsilon(Ca^{2+}, Cl^-)$.
For the data in $Ca(ClO_4)_2$ solution the slope refers to:
$s = -(2/3)\ \varepsilon(Ca_3[Zr(OH)_6]^{4+}, ClO_4^-) + 2 \times (1/3)\ \varepsilon(OH^-, Ca^{2+}) + 3 \times (2/3)\ \varepsilon(Ca^{2+}, ClO_4^-)$.

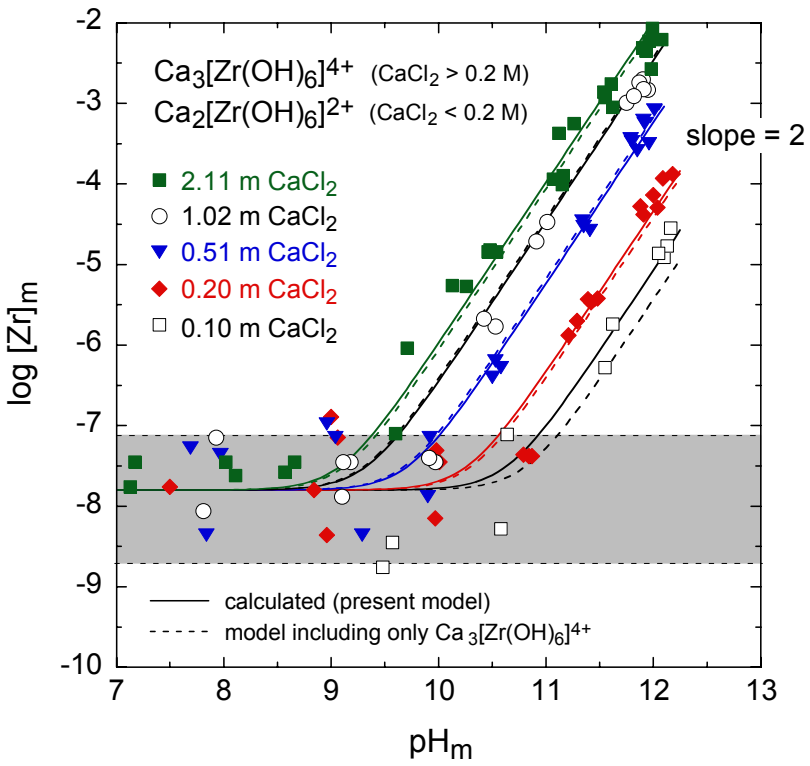

Fig. 4. Solubility of $ZrO_2{\cdot}xH_2O(s)$ in alkaline $CaCl_2$ solutions. The solid lines are calculated with the data in Tables 1 and 2 including both $Ca_2[Zr(OH)_6]^{2+}$ and $Ca_3[Zr(OH)_6]^{4+}$. The dashed lines are based on a model including only the complex $Ca_3[Zr(OH)_6]^{4+}$ (see text).

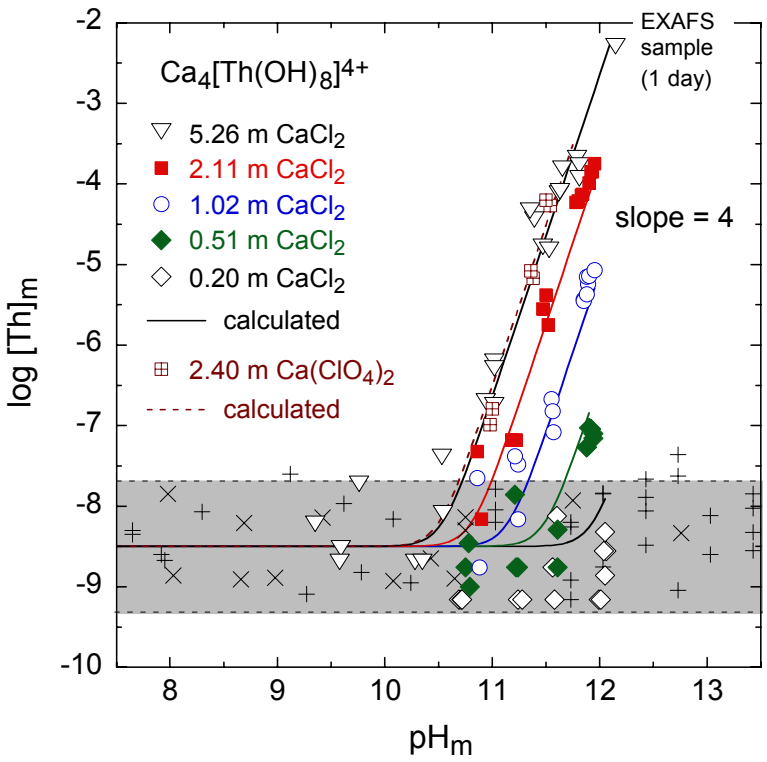

Fig. 5. Solubility of $ThO_2 \cdot xH_2O(s)$ in alkaline $CaCl_2$ (and $Ca(ClO_4)_2$) solutions. Experimental data determined after ultrafiltration or ultracentrifugation in $NaClO_4$, NaCl, and KCl solutions [7, 25-27] are shown as crosses. The solid lines are calculated with $\log K°_{s,(4,1,8)} = 1.8 \pm 0.5$ and $\varepsilon(Ca_4[Th(OH)_8]^{4+}, Cl^-) = -0.01$ and $\varepsilon(Ca_3[Zr(OH)_6]^{4+}, ClO_4^-) = 0.21$ kg·mol^{-1}. Shadowed grey areas are regions of constant Th concentration in calcium-free solutions.

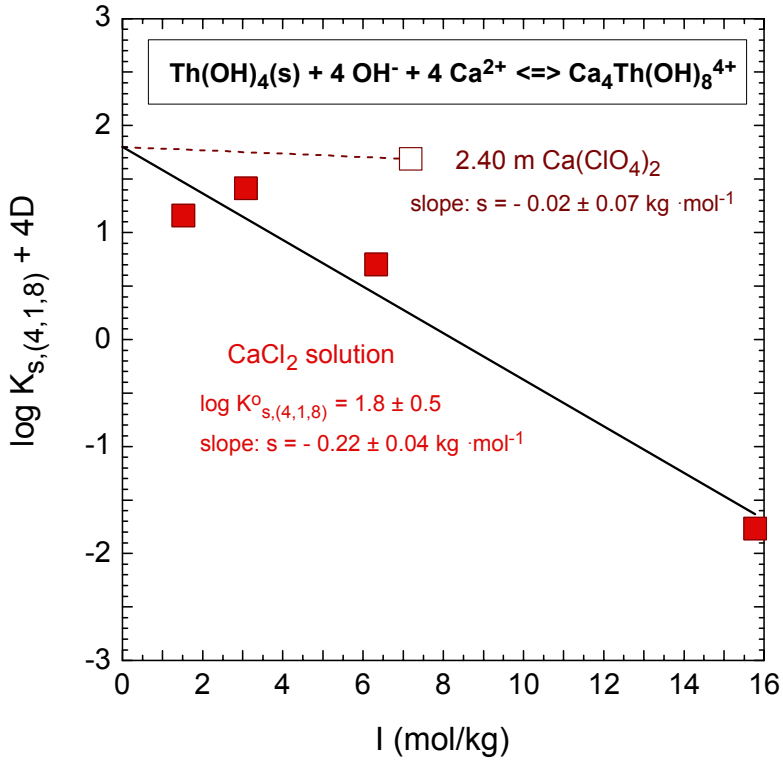

Fig. 6. Application of the linear SIT regression to evaluate the equilibrium constant at I = 0 for the reaction $Th(OH)_4(am) + 4\ Ca^{2+} + 4\ OH^- \Leftrightarrow Ca_4[Th(OH)_8]^{4+}$. Since $m_{Ca^{2+}} = m_{CaCl2} = (1/3)\ I_m$ and $m_{Cl^-} = 2\ m_{CaCl2} = (2/3)\ I_m$ the slope s = - 0.22 ± 0.04 kg·mol^{-1} in the plot of ($\log K_{s,(4,1,8)} + 4D$) vs I_m is related to the individual SIT coefficients by:
$s = -(2/3)\ \varepsilon(Ca_4[Th(OH)_8]^{4+}, Cl^-) + 4 \times (1/3)\ \varepsilon(OH^-, Ca^{2+}) + 4 \times (2/3)\ \varepsilon(Ca^{2+}, Cl^-)$;
$Ca(ClO_4)_2$ solution: slope s = - 0.02 ± 0.07 kg·mol^{-1} = $-(2/3)\ \varepsilon(Ca_4[Th(OH)_8]^{4+}, ClO_4^-) + 4 \times (1/3)\ \varepsilon(OH^-, Ca^{2+}) + 4 \times (2/3)\ \varepsilon(Ca^{2+}, ClO_4^-)$.

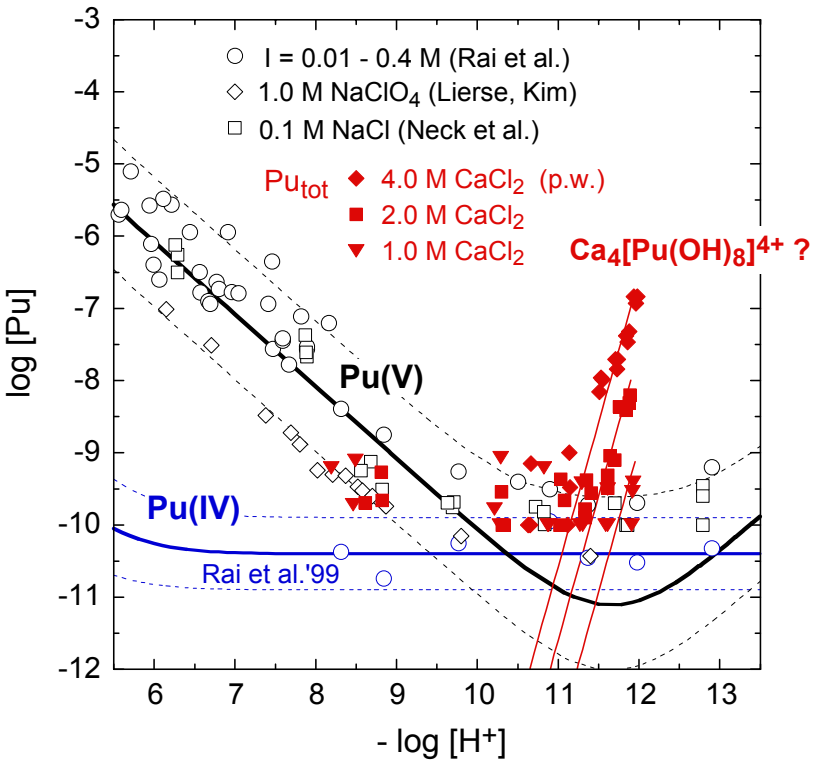

Fig. 7. Solubility of PuO_{2+x}(am,hyd) in alkaline $CaCl_2$ solutions under Ar atmosphere in comparison with experimental data in NaCl [16], $NaClO_4$ [28-31], and KOH [8] solutions. The fat solid lines represent equilibrium Pu(IV) and Pu(V) concentrations as described in [16]. The thin dashed lines are calculated with $\log K°_{s,(4,1,8)} = -2.0$ and $\varepsilon(Ca_4[Pu(OH)_8]^{4+}, Cl^-) = -0.01 \pm 0.10$ kg·mol^{-1}.

Figure captions

Fig. 1.
Experimental pH_m values in $CaCl_2$ matrix solutions equilibrated for about one week (circles: 2 - 3 hours) with calcium hydroxide and/or hydroxychlorides; equilibrium pH_m values calculated with the thermodynamic data and parameters of Harvie et al. [15] are shown as solid lines.

Fig. 2.
Solubility of $ZrO_2 \cdot xH_2O(s)$ in NaCl, $NaClO_4$ (data from [5,6]), $CaCl_2$ and $Ca(ClO_4)_2$ solutions of comparable ionic strength: a) I = 0.5 - 0.6 M, b) I = 1.0 - 1.5 M, and c) I = 3.0 M. The fat lines (solid lines for NaCl and $CaCl_2$, dashed lines for $NaClO_4$ and dotted lines for $Ca(ClO_4)_2$ solutions) are calculated for $\log{}^*K^\circ_{s,0}$ = - 4.3 with the equilibrium constants and SIT coefficients in Tables 1 and 2. The upper and lower thin dashed lines refer to $NaClO_4$ solutions and solids with $\log{}^*K^\circ_{s,0}$ = - 3.7 and - 5.0, respectively.

Fig. 3.
Application of the linear SIT regression to evaluate the equilibrium constant at I = 0.

a) Reaction: $Zr(OH)_4(s) + 2\ OH^- \Leftrightarrow Zr(OH)_6^{2-}$. The slope s in the plot of ($\log K_{s,6}$ - 2D) vs I_m, s = 0.10 ± 0.03 $kg \cdot mol^{-1}$ for data in NaCl and - 0.02 ± 0.01 $kg \cdot mol^{-1}$ for data in pure NaOH solutions (conversion factors m_{NaOH}/c_{NaOH} are taken from [24]), is related to the individual SIT coefficients by: $s = -\Delta\varepsilon = -\varepsilon(Zr(OH)_6^{2-}, Na^+) + 2\ \varepsilon(OH^-, Na^+)$.

b) Reaction: $Zr(OH)_4(s) + 3\ Ca^{2+} + 2\ OH^- \Leftrightarrow Ca_3[Zr(OH)_6]^{4+}$ in $CaCl_2$ solutions.
Since $m_{Ca2+} = m_{CaCl2} = (1/3)\ I_m$ and $m_{Cl-} = 2\ m_{CaCl2} = (2/3)\ I_m$ the slope s = - 0.34 ± 0.05 $kg \cdot mol^{-1}$ in the plot of ($\log K_{s,(3,1,6)}$ - 2D) vs I_m is related to the individual SIT coefficients by:
$s = -(2/3)\ \varepsilon(Ca_3[Zr(OH)_6]^{4+}, Cl^-) + 2 \times (1/3)\ \varepsilon(OH^-, Ca^{2+}) + 3 \times (2/3)\ \varepsilon(Ca^{2+}, Cl^-)$.
For the data in $Ca(ClO_4)_2$ solution the slope refers to: $s = -(2/3)\ \varepsilon(Ca_3[Zr(OH)_6]^{4+}, ClO_4^-) + 2 \times (1/3)\ \varepsilon(OH^-, Ca^{2+}) + 3 \times (2/3)\ \varepsilon(Ca^{2+}, ClO_4^-)$.

Fig. 4.
Solubility of $ZrO_2 \cdot xH_2O(s)$ in alkaline $CaCl_2$ solutions. The solid lines are calculated with the data in Tables 1 and 2 including both $Ca_2[Zr(OH)_6]^{2+}$ and $Ca_3[Zr(OH)_6]^{4+}$. The dashed lines are based on a model including only the complex $Ca_3[Zr(OH)_6]^{4+}$ (see text).

Fig. 5.

Solubility of $ThO_2 \cdot xH_2O(s)$ in alkaline $CaCl_2$ (and $Ca(ClO_4)_2$) solutions. Experimental data determined after ultrafiltration or ultracentrifugation in $NaClO_4$, NaCl, and KCl solutions [7, 25-27] are shown as crosses. The solid lines are calculated with $\log K°_{s,(4,1,8)} = 1.8 \pm 0.5$ and $\varepsilon(Ca_4[Th(OH)_8]^{4+}, Cl^-) = -0.01$ and $\varepsilon(Ca_3[Zr(OH)_6]^{4+}, ClO_4^-) = 0.21$ kg·mol^{-1}. Shadowed grey areas are regions of constant Th concentration in calcium-free solutions.

Fig. 6.

Application of the linear SIT regression to evaluate the equilibrium constant at I = 0 for the reaction $Th(OH)_4(am) + 4\ Ca^{2+} + 4\ OH^- \Leftrightarrow Ca_4[Th(OH)_8]^{4+}$. Since $m_{Ca^{2+}} = m_{CaCl2} = (1/3)\ I_m$ and $m_{Cl^-} = 2\ m_{CaCl2} = (2/3)\ I_m$ the slope s = - 0.22 ± 0.04 kg·mol^{-1} in the plot of ($\log K_{s,(4,1,8)}$ + 4D) vs I_m is related to the individual SIT coefficients by:

$s = -(2/3)\ \varepsilon(Ca_4[Th(OH)_8]^{4+}, Cl^-) + 4 \times (1/3)\ \varepsilon(OH^-, Ca^{2+}) + 4 \times (2/3)\ \varepsilon(Ca^{2+}, Cl^-)$;

$Ca(ClO_4)_2$ solution: slope s = - 0.02 ± 0.07 kg·mol^{-1} = $-(2/3)\ \varepsilon(Ca_4[Th(OH)_8]^{4+}, ClO_4^-) + 4 \times (1/3)\ \varepsilon(OH^-, Ca^{2+}) + 4 \times (2/3)\ \varepsilon(Ca^{2+}, ClO_4^-)$.

Fig. 7.

Solubility of $PuO_{2+x}(am,hyd)$ in alkaline $CaCl_2$ solutions under Ar atmosphere in comparison with experimental data in NaCl [16], $NaClO_4$ [28-31], and KOH [8] solutions. The fat solid lines represent equilibrium Pu(IV) and Pu(V) concentrations as described in [16]. The thin dashed lines are calculated with $\log K°_{s,(4,1,8)} = -2.0$ and $\varepsilon(Ca_4[Pu(OH)_8]^{4+}, Cl^-) = -0.01 \pm 0.10$ kg·mol^{-1}.